

Magnetization transfer contrast MRI in GFP-tagged live bacteria

VALERIA RIGHI¹⁻³, MELISSA STARKEY^{4,5}, GEORGE DAI², LAURENCE G. RAHME⁴ and ARIA A. TZIKA^{1,2}

¹NMR Surgical Laboratory, Department of Surgery, Massachusetts General Hospital and Shriners Burns Hospital, Harvard Medical School; ²Department of Radiology, Massachusetts General Hospital, Harvard Medical School, Athinoula A. Martinos Center for Biomedical Imaging, Boston, MA 02114, USA; ³Department of The Quality of Life Science, University of Bologna, Rimini, RN I-47921, Italy; ⁴Molecular Surgery Laboratory, Department of Surgery, Massachusetts General Hospital and Shriners Burns Institute, Harvard Medical School, Boston, MA 02114; ⁵American College of Physicians, Philadelphia, PA 19106, USA

Received December 28, 2017; Accepted May 22, 2018

DOI: 10.3892/mmr.2018.9669

Abstract. Green fluorescent protein (GFP) is a widely utilized molecular reporter of gene expression. However, its use in *in vivo* imaging has been restricted to transparent tissue mainly due to the tissue penetrance limitation of optical imaging. Magnetization transfer contrast (MTC) is a magnetic resonance imaging (MRI) methodology currently utilized to detect macromolecule changes such as decrease in myelin and increase in collagen content. MTC MRI imaging was performed to detect GFP in both *in vitro* cells and in an *in vivo* mouse model to determine if MTC imaging could be used to detect infection from *Pseudomonas aeruginosa* in murine tissues. It was demonstrated that the approach produces values that are protein specific and concentration dependent. This method provides a valuable, non-invasive imaging tool to study the impact of novel antibacterial therapeutics on bacterial proliferation and perhaps viability within the host system, and could potentially suggest the modulation of bacterial gene expression within the host when exposed to such compounds.

Introduction

Pseudomonas aeruginosa (*P. aeruginosa*) is one of the ESKAPE bacterial species that is particularly concerning, because they represent the largest group of nosocomial pathogens with growing incidences of antibiotic resistance (1,2). Plethora of studies are focused on eliminating or reducing *P. aeruginosa* infection by using novel molecules (3-5). The main problem is tracking the action of these molecules

in vivo, with a non-invasive method. Magnetic resonance imaging (MRI) can be considered as a non-invasive method for monitoring the course of the infection. An MRI approach using USPIO nanoparticles as molecules to label the macrophages that are present in the infected area has been reported and seems to open perspectives for testing novel anti-infective compounds (6,7). Recently, the explosion in available fluorescent proteins promises a wide variety of new tools for biological imaging, and in particular, for protein labeling and cell tracing (8). In the last decade, Green Fluorescent Protein (GFP) has been frequently used as a marker of gene expression, since it is non-toxic for both animals and bacteria and thus useful for *in vivo* imaging (9). The introduction of GFP has revolutionized the field of cell biology and fluorescence microscopy (10). GFP is a naturally fluorescent protein, consisting of an 11-strand β -barrel wrapped around a central helix that is widely utilized as a fluorescent marker of gene expression (11). GFP is detected by optical spectroscopy through its fluorescent properties; the protein has a major excitation peak at 395 nm and in a normal solution gives emission peaking at 508 nm (11). *In vivo* GFP can be detected only if the tissue is transparent or if protein expression is close to tissue surface (12). Due to this limitation, most experiments utilizing this marker are focused on *in vitro* cell cultures, *ex vivo* histology slices, or transparent animal models (13,14).

GFP is extensively used in animal models, in transplantation studies to determine the fate of transplanted cells, as well as for studying various biological processes. Published studies on *in vivo* MRI using GFP protein as a marker to label tumor cells for example melanoma cells (15) or stem cells (16) suggested that the labeling does not affect expression of other genes.

Recently, the magnetization transfer contrast (MTC) technique was used to detect GFP and was shown to produce protein-specific values that seemed to be concentration dependent (17). MTC MRI has been utilized for detecting early macromolecular changes in the Tg2576 mouse model of Alzheimer's disease (18) for localizing the signal to noise ratio (SN) *in vivo* (19). MTC is an MRI technique able to detect changes in macromolecule concentration and composition (20). MTC is commonly used to track changes in myelination as a

Correspondence to: Dr Aria A. Tzika, NMR Surgical Laboratory, Department of Surgery, Massachusetts General and Shriners Burns Hospitals, Harvard Medical School, 51 Blossom Street, Room 261, Boston, MA 02114, USA
E-mail: atzika@hms.harvard.edu

Key words: magnetization transfer contrast imaging, green fluorescent protein, *Pseudomonas aeruginosa*, burn mouse model, *in vitro* cells, *in vivo* mouse

way to grade multiple sclerosis lesions (21). Recently, MTC has also been utilized to detect macromolecular accumulation in a mouse model of early Alzheimer's disease (18).

The MTC technique uses the application of a radiofrequency pulse at a specific distance from the water resonance, known as the offset frequency. This radiofrequency pulse causes a loss of signal intensity proportional to macromolecular concentration. When combined with a reference image, where the radiofrequency pulse is not applied, the percent of signal loss can be quantified in what is referred to as the magnetization transfer ratio (MTR). Specifically, MTC evaluates changes in semisolid macromolecules (22).

This provides a flexible, non-invasive *in vivo* molecular imaging system exclusively dependent on the concentration of the fluorescent reporter. Starting from these results the idea of this work was the possibility to follow the *P. aeruginosa* infection *in vivo* using the MTC MRI method and the GFP as a molecular marker.

Materials and methods

Bacterial strains and growth conditions. UCBPP-PA14 (PA14) is a *P. aeruginosa* human clinical isolate (23). GFP-tagged *P. aeruginosa* (PA-GFP), (Fig. 1), GFP-tagged *E. coli* (EC-GFP) (both tagged with a stable plasmid expressing GFP) and non-fluorescent *P. aeruginosa* (PA) cells were grown overnight in 5 ml LB Lenox medium (Thermo Fisher Scientific, Inc., Waltham, MA, USA) at 37°C under 200 rpm orbital shaking using glass tubes (VWR). The next day, bacteria were centrifuged, re-suspended and diluted in phosphate-buffered saline (PBS) to final concentrations of 5×10^6 and 5×10^5 cells/ml. The latter concentration is equivalent to the PA inoculum used in a murine burn and infection model. Then 0.2 ml microfuge tubes were filled to the maximum capacity with the diluted cultures (23). Fluorescence of the cells was confirmed by microscopy under the 1st section talking about the bacteria.

Phantom. One phantom was prepared to test and calibrate the experiments. Three microfuge tubes (capacity 0.2 ml) were filled to the maximum capacity with the diluted cultures of PA-GFP, EC-GFP and PA cells, respectively, and placed in a Falcon tube (2.7 cm inner diameter) filled with isotonic saline (NaCl) solution.

Animals. Six weeks old, CD-1 mice were anesthetized and a leg burn injury of 5% total burn surface area (TBSA) was produced on the right thigh muscle. Briefly, animals were anesthetized with Xylazine (13 mg/kg, i.p.) and Ketamine (87 mg/kg, i.p.), thermally injured (5-8% of body surface) on the shaved abdomen dermis, and intra-dermally infected into the burn eschar. Mice were randomized into one experimental and control groups (N=6 per group). The experimental group consisted of burned mice infected with PA-GFP-tagged PA14 *P. aeruginosa* strain containing no plasmid and the control group consisted of burned mice infected with wild-type *P. aeruginosa*. Mice were infected as described in Rahme *et al* (23). An inoculum of 5×10^5 PA14 cells in 100 μ l of PBS was injected intradermal into the burn eschar. The animal protocol was approved by the Massachusetts General Hospital Institutional Animal Care and Use Committee.

MRI experiments. The mice were imaged 12 h post-burn and infection. During MRI, mice were kept anesthetized with a mixture of isoflurane and maintained at 37°C.

We used a triple phantom in a 4.7 T horizontal bore magnet (20 cm bore diameter, Magnex Scientific, using a Bruker Avance console). The images were acquired in a 4.7 T horizontal magnet, 20 cm bore, equipped with gradient system capable of 39 G/cm, Magnex Scientific, using a Bruker Avance console (Bruker BioSpin, Billerica, MA, USA) with a custom-built volume coil of 3 cm inner diameter and 10 cm active length. The main magnetic field (B0) was shimmed and the RF field (B1) was calibrated. We acquired a RARE sequence (also known as Fast Spin Echo, FSE) with magnetization transfer (24-26). The imaging pulse sequence comprised a pre-saturation pulse at the designated offset frequency followed by a spin echo sequence with TE/TR=7.95/2,000 msec. Images were recorded with a 128x128 matrix, field of view, 3x3 cm; slice thickness, 3 mm; and average, 1. Pre-saturation off-resonance pulses ranged from ± 0.05 to ± 0.4 kHz.

Magnetization transfer ratios (MTR) in the form of $MTR = (\text{unsaturated} - \text{saturated}) / \text{unsaturated}$ were calculated from the signal intensities of regions of interest (ROI) using Paravision software (Bruker BioSpin).

Statistical analysis. Data are expressed as a mean \pm standard deviation. Comparisons between groups were performed in each group using a two-tailed t-test (P-value=0.05). Moreover we implemented the analysis with a One-Way ANOVA analysis followed by Tukey's post hoc test using the Metaboanalyst online software (<http://www.metaboanalyst.ca/>).

Results

GFP cell model. We compared the MTC profiles of GFP-tagged *P. aeruginosa* cells to those of the non-fluorescent *P. aeruginosa*, GFP-tagged and *E. coli* cells in culture. Cells were visualized in 0.2 ml tubes filled to capacity with 5×10^5 cells/ml. The non-fluorescent *P. aeruginosa*, was chosen as a non-specific control to compare against GFP-tagged bacteria, whereas *E. coli* was used as a specific control for the GFP to compare with both tagged and wild-type *P. aeruginosa*. The goal was to find the frequency at which there was the largest difference between GFP-tagged *P. aeruginosa* and *E. coli*, and non-fluorescent *P. aeruginosa* (Fig. 2). Samples were imaged first without and then with MTC. Nine MTC datasets were acquired from 0.05 to 0.4 kHz. The MTR was calculated from the images, and is shown in Fig. 3A. We found the largest difference between 0.2, 0.25 and 0.3 kHz (the peak difference was at 0.25 kHz) for EC-GFP and for PA-GFP with respect to PA (Fig. 3A). Pseudo-colored pixel by pixel MTR calculations visually show a clear difference between the PA-GFP and PA phantoms (Fig. 3B); we found a statistically significant difference between PA and EC-GFP ($P < 0.0001$), and an even greater statistically significant difference between PA and PA-GFP ($P = 0.00001$). These simple t-test analysis is confirmed by using a multiple comparison Tukey's analysis (One-way ANOVA Analysis). The PA samples are strongly different from EC-GFP and PA-GFP and the data are statistically significant with $P < 0.001$ and $P < 0.01$ respectively.

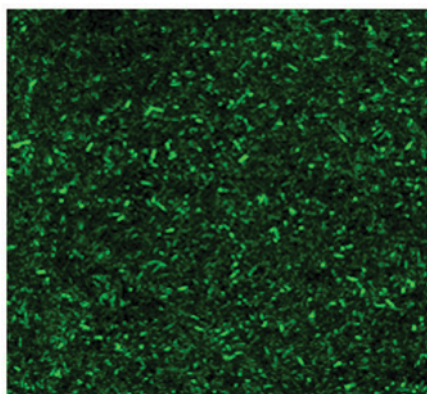


Figure 1. GFP-tagged *Pseudomonas aeruginosa* cells viewed at x600 magnification. GFP, green fluorescent protein.

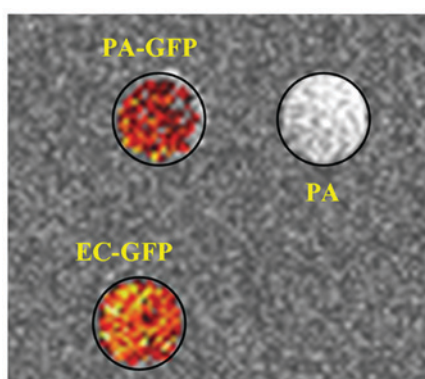


Figure 2. Pseudocolored pixel of *EC-GFP*, *PA-GFP* and *PA* at 0.25 kHz offset. GFP, green fluorescent protein; *EC-GFP*, GFP-tagged *E. coli*; *PA-GFP*, GFP-tagged *Pseudomonas aeruginosa*.

GFP mouse model. The comparison of the GFP-tagged and non-tagged live *P. aeruginosa* and *E. coli* cells using MTC MRI indicated that this method was sensitive enough to distinguish between GFP-tagged and non-tagged bacteria at cell concentrations relevant to those to be used in animal infection models. Accordingly, the MTC MRI profiles of mice infected with non-tagged *P. aeruginosa* and mice infected with GFP-tagged *P. aeruginosa* were compared to determine the frequency with the largest difference between them in the infected a burn area. Fig. 4 shows the *in vivo* MRI results from our experiments in mice, and the MTR maps demonstrated an enhancement in the GFP expressing infected animals. The two groups (GFP-positive and GFP-negative) were imaged first without and then with MTC. In addition, nine MTC datasets were acquired from 0.2 to 1.6 kHz. The control animal did not give any appreciable signal at this setting. The MTR was calculated from the images, and is shown in Fig. 5A. We found the largest difference between 0.8, 1 and 1.2 kHz, the peak difference being at 1 kHz, for the GFP-positive with respect to the GFP-negative mice. Fig. 5B shows the calculated MTR values; we found a statistically significant difference between GFP⁺ and GFP⁻ with a $P < 0.0001$.

The visual representation is more useful to assess the spatial distribution of signal changes compared to a single ROI analysis. The unsaturated images for a representative GFP expressing and control animal demonstrated different signal

intensities. The MTR maps demonstrated an enhancement in the GFP expressing animals.

Discussion

MTC MRI methods have been used before to distinguish intrinsic macromolecule concentration changes. The main advantages of detecting GFP, an extrinsic protein marker, with MTC MRI compared to other MRI based reporters, such as USPIO are the non-toxicity of the protein and the potential to detect the expression of a specific gene or product *in vivo* serially and non-invasively. Our results confirm that we can detect GFP-tagged live bacteria using MTC MRI both *in vitro* and *in vivo*.

Comparison of the GFP-tagged and non-tagged live *P. aeruginosa* and *E. coli* cells using the MTC MRI methodology indicated that this method was sensitive enough to distinguish between GFP-tagged and non-tagged bacteria and to successfully image *in vivo* GFP-tagged *P. aeruginosa* in a non-invasive manner. We observed a difference in the MRI MTR value between *PA* and *PAGFP*, which was statistically significant ($P < 0.0001$).

Also, we report an *in vivo* study of GFP-tagged MTC MRI in a burn mouse model infected with *P. aeruginosa*. The utility of this method is to visualize bacterial infections *in vivo* in real time, and to study the impact of novel therapeutics on bacterial proliferation and viability within the host system. The use of an extrinsic protein marker provides an added flexibility. The main advantages of detecting GFP with MTC MRI over other MRI based reporters includes that there are multiple GFP mouse lines available and it poses no toxicity to the host or the bacteria.

Our results confirm the hypothesis that we can detect GFP-tagged live bacteria using MTC MRI.

The study reported here assessed detection of GFP through MTC MRI both *in vitro* and *in vivo* experiments. To provide optimal results and the best off-set frequency we worked on the fine-tuned and at the end we found that 1 kHz offset as the most robust offset frequency for the MTC detection of GFP and provided the difference between tagged and non-tagged mice. Our results are similar to the data reported by Pérez-Torres *et al* (17).

We were able to successfully use this methodology to image *in vivo* GFP-tagged *P. aeruginosa* in a murine burn and infection model, showing the utility of MTC for tracking bacterial proliferation and gene expression *in vivo* in animal models in a non-invasive manner. The significance of this method is that it can be used to visualize bacterial infections *in vivo* in real time without being restricted to the use of transparent tissue necessary for optical imaging. The innocuous nature of the technology allows for repeated imaging over time without damage to the host or the bacteria. Furthermore, this *in vivo*, MRI molecular imaging technique can detect varying levels of the GFP reporter, further establishing its utility for studying host-bacterial interactions. In addition to the visualizing bacterial infections and expression of GFP tagged gene, *in vivo* and in real time, this method could be suitable for assessing the efficacy of novel therapeutics on specific targets, and, bacterial proliferation and viability within the host system.

Overall, this method provides a valuable, non-invasive imaging tool to study the impact of novel antibacterial

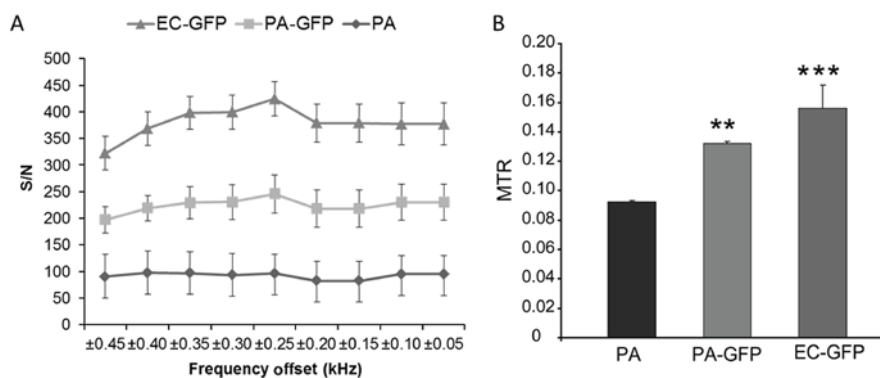


Figure 3. (A) Region based MTR calculations for the different frequency offsets for PA, PA-GFP and EC-GFP from 0.05 to 0.45 kHz (frequency offset). (B) MTR (mean \pm SE) of PA, PA-GFP and EC-GFP. Data were analyzed using one-way ANOVA analysis followed by Tukey's post hoc test. ** $P < 0.01$ and *** $P < 0.001$ vs. PA. PA, *Pseudomonas aeruginosa*; GFP, green fluorescent protein; EC-GFP, GFP-tagged *E. coli*; PA-GFP, GFP-tagged *Pseudomonas aeruginosa*; MTR, magnetization transfer ratio.

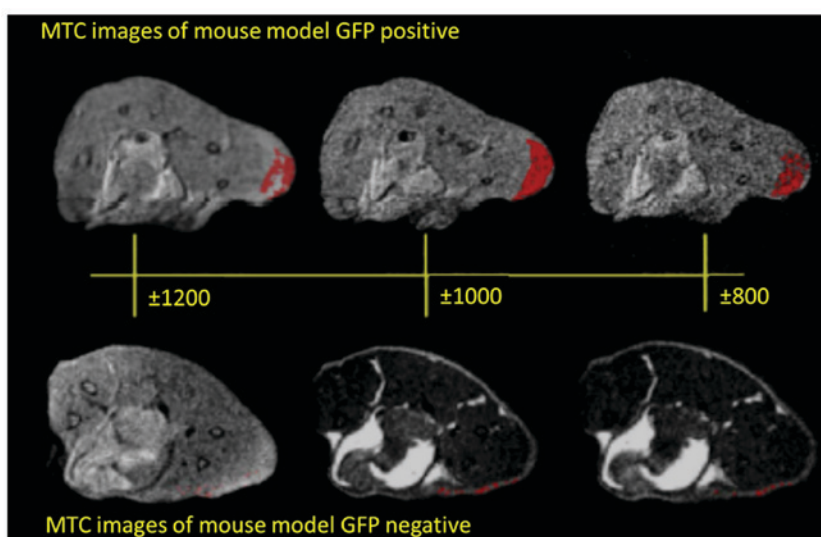


Figure 4. Pseudocolored pixel of GFP⁺ (upper) and GFP⁻ (lower) mice MR images at 1 kHz offset. GFP, green fluorescent protein.

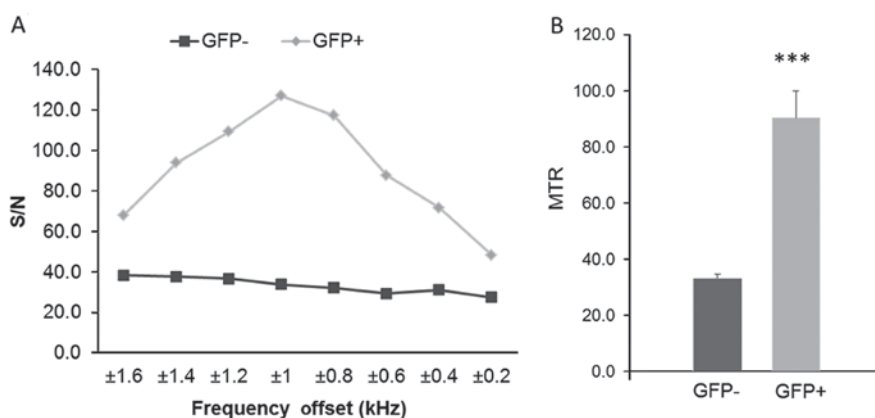


Figure 5. (A) Region based MTR calculations for the different frequency offsets for mice GFP⁻ and mice GFP⁺ from 0.2 to 1.6 kHz (frequency offset). (B) MTR (mean \pm SE) of GFP⁻ and GFP⁺, P-values. *** $P < 0.0001$ vs. GFP⁻. GFP, green fluorescent protein; MTR, magnetization transfer ratio.

therapeutics on bacterial proliferation and perhaps viability within the host system, and could potentially give clues to the modulation of bacterial gene expression within the host when exposed to such compounds.

Acknowledgements

This abstract was presented at the International Society of Magnetic Resonance Annual Meeting held in Stockholm in 2010

and was published as Abstract no. 5135 Proceeding 'Righi V, Starkey M, Dai G, Rahme LG and Tzika AA: Magnetization transfer contrast MRI in GFP-tagged live bacteria. Proc Intl Soc Mag Reson Med 18: 513, 2010. ISBN: 978-1-61782-008-3'. This abstract was presented at the International Society of Magnetic Resonance Annual Meeting hold in Montreal in 2011 and was published as Abstract no. 662 Proceeding 'Righi V, Starkey M, Rahme LG, Tompkins RG and Tzika AA: Magnetization Transfer Contrast MRI detects *Pseudomonas Aeruginosa* bacterial infection a mouse burn model. Proc Intl Soc Mag Reson Med 19: 662, 2011. ISBN: 978-1-61839-284-8. ISSN: 1545-4428'.

Funding

The present study was funded by Shriners Burn Hospitals and NIH grants (NIH grant no. R01AI134857 and grant no. R33AI105902).

Availability of data and materials

All data generated or analysed during this study are included in this published article.

Authors' contributions

VR analyzed the samples and interpreted data and wrote the manuscript; MS prepared the samples and helped in writing the manuscript; GD helped in the MRI acquisition data; LR supported the study, helped in writing the manuscript and interpreting the results, and organized the cells and mice preparation, AT designed the study, helped in data interpretation and wrote the manuscript. All authors read and approved the final manuscript.

Ethics approval and consent to participate

This study was carried out in strict accordance with the recommendations of the Guide for the Care and Use of Laboratory Animals of the National Institutes of Health. The protocol was approved by the Committee on the Ethics of Animal Experiments at Massachusetts General Hospital (Permit no. 2006N000093/2).

Patient consent for publication

Not applicable.

Competing interests

The authors declare that they have no competing interests.

References

1. Turner KH, Everett J, Trivedi U, Rumbaugh KP and Whiteley M: Requirements for *Pseudomonas aeruginosa* acute burn and chronic surgical wound infection. *PLoS Genet* 10: e1004518, 2014.
2. Pendleton JN, Gorman SP and Gilmore BF: Clinical relevance of the ESKAPE pathogens. *Expert Rev Anti Infect Ther* 11: 297-308, 2013.
3. Church D, Elsayed S, Reid O, Winston B and Lindsay R: Burn wound infections. *Clin Microbiol Rev* 19: 403-434, 2006.
4. Lyczak JB, Cannon CL and Pier GB: Establishment of *Pseudomonas aeruginosa* infection: Lessons from a versatile opportunist. *Microbes Infect* 2: 1051-1060, 2000.
5. McVay CS, Velásquez M and Fralick JA: Phage therapy of *Pseudomonas aeruginosa* infection in a mouse burn wound model. *Antimicrob Agents Chemother* 51: 1934-1938, 2007.
6. Andronesi OC, Mintzopoulos D, Righi D, Psychogios N, Kesarwani M, He J, Yasuhara S, Dai G, Rahme LG and Tzika AA: Combined off-resonance imaging and T2 relaxation in the rotating frame for positive contrast MR imaging of infection in a murine burn model. *J Magn Reson Imaging* 32: 1172-1183, 2010.
7. Starkey M, Lepine F, Maura D, Bandyopadhyaya A, Lesic B, He J, Kitao T, Righi V, Milot S, Tzika A and Rahme L: Identification of anti-virulence compounds that disrupt quorum-sensing regulated acute and persistent pathogenicity. *PLoS Pathog* 10: e1004321, 2014.
8. Shaner NC, Steinbach PA and Tsien RY: A guide to choosing fluorescent proteins. *Nat Methods* 2: 905-909, 2005.
9. Chalfie M, Tu Y, Euskirchen G, Ward WW and Prasher DC: Green fluorescent protein as a marker for gene expression. *Science* 263: 802-805, 1994.
10. Stepanenko OV, Verkhusha VV, Kuznetsova IM, Uversky VN and Turoverov KK: Fluorescent proteins as biomarkers and biosensors: Throwing color lights on molecular and cellular processes. *Curr Protein Pept Sci* 9: 338-369, 2008.
11. Tsien RY: The green fluorescent protein. *Annu Rev Biochem* 67: 509-544, 1998.
12. Helmchen F and Denk W: Deep tissue two-photon microscopy. *Nat Methods* 2: 932-940, 2005.
13. Shaner NC, Patterson GH and Davidson MW: Advances in fluorescent protein technology. *J Cell Sci* 120: 4247-4260, 2007.
14. Zhang J, Campbell RE, Ting AY and Tsien RY: Creating new fluorescent probes for cell biology. *Nat Rev Mol Cell Biol* 3: 906-918, 2002.
15. Wunderbaldinger P, Josephson L, Bremer C, Moore A, Weissleder R: Detection of lymph node metastases by contrast-enhanced MRI in an experimental model. *Magn Reson Med* 47: 292-297, 2002.
16. Pawelczyk E, Jordan EK, Balakumaran A, Chaudhry A, Gormley N, Smith M, Lewis BK, Childs R, Robey PG and Frank JA: In vivo transfer of intracellular labels from locally implanted bone marrow stromal cells to resident tissue macrophages. *PLoS One* 4: e6712, 2009.
17. Pérez-Torres CJ, Massaad CA, Hilsenbeck SG, Serrano F and Pautler RG: In vitro and in vivo magnetic resonance imaging (MRI) detection of GFP through magnetization transfer contrast (MTC). *Neuroimage* 50: 375-382, 2010.
18. Pérez-Torres CJ, Reynolds JO and Pautler RG: Use of magnetization transfer contrast MRI to detect early molecular pathology in Alzheimer's disease. *Magn Reson Med* 71: 333-338, 2014.
19. Bolding MS, Reid MA, Avsar KB, Roberts RC, Gamlin PD, Gawne TJ, White DM, den Hollander JA and Lahti AC: Magnetic transfer contrast accurately localizes substantia nigra confirmed by histology. *Biol Psychiatry* 73: 289-294, 2013.
20. Wolff SD and Balaban RS: Magnetization transfer contrast (MTC) and tissue water proton relaxation in vivo. *Magn Reson Med* 10: 135-144, 1989.
21. Horsfield MA: Magnetization transfer imaging in multiple sclerosis. *J Neuroimaging* 15 (Suppl 4): 58S-67S, 2005.
22. Henkelman RM, Stanisz GJ and Graham SJ: Magnetization transfer in MRI: A review. *NMR Biomed* 14: 57-64, 2001.
23. Rahme LG, Stevens EJ, Wolfort SF, Shao J, Tompkins RG and Ausubel FM: Common virulence factors for bacterial pathogenicity in plants and animals. *Science* 268: 1899-1902, 1995.
24. Forsén S and Hoffman RA: Study of moderately rapid chemical exchange reactions by means of nuclear magnetic double resonance. *J Chem Phys* 39: 2892, 1963.
25. Baguet E and Roby C: Off-resonance irradiation effect in steady-state NMR saturation transfer. *J Magn Reson* 128: 149-160, 1997.
26. Sun PZ, Van Zijl PC and Zhou J: Optimization of the irradiation power in chemical exchange dependent saturation transfer experiments. *J Magn Reson* 175: 193-200, 2005.